Linker Histones Incorporation Maintains Chromatin Fiber Plasticity

Pierre Recouvreux,[†] Christophe Lavelle,[†‡§] Maria Barbi,[¶] Natalia Conde e Silva,[‖] Eric Le Cam,[‡] Jean-Marc Victor,[¶] and Jean-Louis Viovy[†*]

[†]Institut Curie, Centre National de la Recherche Scientifique UMR 168, Université Pierre et Marie Curie, Paris, France; [‡]Institut Gustave Roussy, Centre National de la Recherche Scientifique UMR 8126, Villejuif, France; [§]Muséum National d'Histoire Naturelle, Centre National de la Recherche Scientifique UMR 7196, INSERM U565, Paris, France; [¶]Laboratoire de Physique Théorique de la Matière Condensée, Centre National de la Recherche Scientifique UMR 7600, Paris, France; and [‖]Institut Jacques Monod, Centre National de la Recherche Scientifique UMR 7592, Paris, France

ABSTRACT Genomic DNA in eukaryotic cells is organized in supercoiled chromatin fibers, which undergo dynamic changes during such DNA metabolic processes as transcription or replication. Indeed, DNA-translocating enzymes like polymerases produce physical constraints in vivo. We used single-molecule micromanipulation by magnetic tweezers to study the response of chromatin to mechanical constraints in the same range as those encountered in vivo. We had previously shown that under positive torsional constraints, nucleosomes can undergo a reversible chiral transition toward a state of positive topology. We demonstrate here that chromatin fibers comprising linker histones present a torsional plasticity similar to that of naked nucleosome arrays. Chromatosomes can undergo a reversible chiral transition toward a state of positive torsion (reverse chromatosome) without loss of linker histones.

INTRODUCTION

Chromatin is constantly changing its structure to accommodate and regulate DNA transcription, replication, recombination, and repair. As DNA-translocating enzymes such as polymerases pull and twist DNA, transient physical constraints propagate through chromatin fibers (1,2). The recent development of experimental tools allowing single molecule manipulation has enabled the investigation of individual chromatin fibers, leading to remarkable progress in the knowledge of the structure and dynamics of this ubiquitous nucleoprotein complex. The response of single chromatin fibers to tension (3–7) or torsion (8,9) has revealed the very high resilience of chromatin, and its ability to reversibly undergo considerable extensional and rotational deformations under moderate stress constraints, well in the range of those exerted by DNA-associated enzymes.

In earlier work, we quantitatively investigated the torsional resilience of regular nucleosome arrays, and showed that it could be explained by a dynamic equilibrium between three conformations of the nucleosome, corresponding to different crossing geometries adopted by DNA as it enters and exits the nucleosome (8). These states are known as negative crossed, open, and positive crossed. In a second study, we showed that chromatin fibers undergo no nucleosome loss after extensive positive supercoiling, but, under such conditions, they display an hysteretic behavior in their mechanical response to torsion (9). This hysteresis was interpreted as a consequence of the trapping of positive turns in individual nucleosomes through their transition to an altered form called a reversome (for reverse nucleosome), which can be related to the previously documented chiral transition of the tetrasome (10).

A recent article also suggested that centromeric nucleosomes spontaneously adopt conformations inducing positive supercoiling both in vivo and when assembled in vitro thanks to the yeast chaperone RbAp48 (11). It was suggested that it could be associated with kinetochore recruitment, and maintenance of centromere localization on the chromosome. Overall, recent evidence converges to suggest that the supercoiling of DNA in chromatin has a major and very specific biological relevance, even if its role is far from being fully elucidated.

Among pending questions, the influence of linker histones on these unusual topological states has not been investigated so far. One histone of this family per nucleosome is thought to join, in vivo, the two nucleosomal DNA-ends in a stem motif (12,13), reducing mononucleosome thermal breathing while at the same time facilitating conformational fluctuations between positively crossed and negatively crossed states (14,15). More precisely, linker histone association suppresses the open conformation, but also changes topologies of negative and positive states, leading to a lower (respectively, higher) value for negative (respectively, positive) conformation. Thus, a change in the individual topology and a change in distribution between the two states (related to difference in energy between topological states) lead to a change in mean topological deformation. In vitro experiments performed so far did not involve linker histones, and to our knowledge, the presence of linker histone in centromeric chromatin is also unknown.

Thus, we decided to address here the influence of linker histones on the torsional plasticity of chromatin. Rather surprisingly, we discovered that chromatosomal and nucleosomal templates respond to torsional constraints in a rather

Submitted November 17, 2010, and accepted for publication March 24, 2011.

*Correspondence: jean-louis.viovy@curie.fr

Editor: Laura Finzi.

0006-3495/11/06/2726/10 $2.00

doi: 10.1016/j.bpj.2011.03.064

similar fashion, suggesting that chromatin resilience does not change significantly upon linker histone binding.

MATERIALS AND METHODS

Nucleosome and chromatosome arrays preparation

Nucleosomes were reconstituted on ultrapositioning sequences 601. We purified a plasmid containing 19 tandem repeats of 200-bp 601 sequences (gift from D. Rhodes). This 3800-bp sequence was extracted before a dimerization leading to a 38 × 200-bp 601 sequence. The DNA construct we used consisted of five fragments ligated to each other. Central fragment was the 38 × 200-bp 601 positioning sequence, flanked by a spacer DNA and extended at each extremity by a sticking DNA. Spacer DNAs were prepared by PCR amplification using the pFos DNA template. To attach the construct to the glass coverslide, 600-bp sticking DNAs were labeled with digoxigenin (dig-modified dUTP from Roche Applied Science, Basel, Switzerland). The attachment to the paramagnetic bead coated with streptavidin is mediated by a 600-bp DNA ligated at the other extremity. This sticking DNA fragment is labeled with biotin (biotin-modified dUTP from Roche Applied Science). These two fragments were prepared by PCR amplification using Litmus 28i DNA as a template.

Nucleosome arrays were prepared by conventional stepwise dilution (16). Core histones from duck erythrocytes are mixed with DNA at a sodium chloride concentration of 2 M. Successive steps correspond to a sodium chloride concentration of 2 M (15 min), 1 M (30 min), 0.8 M (1 h), 0.6 M (2 h), and 0.4 M (1 h) followed by a dialysis against TE buffer (Tris 10 mM, EDTA 1 mM). Nucleosome occupancy was checked by gel electrophoresis and electron microscopy. Chromatosome assembly followed the same protocol except for the fact that linker histone H5 is added in the solution when NaCl concentration is 0.4 M. Fibers were stored at −20°C in buffer B0 (10 mM Tris + 1 mM EDTA + 0.1 mg/mL BSA, pH = 7.5) diluted onefold with 100% glycerol (v/v).

Fit of the experimental results

The hysteresis cycles are modeled according to the following line of arguments:

1. We assume four different configurations, or states, for the nucleosome. The first three states correspond to the standard nucleosome and are only differentiated by conditions on the entry/exit linker DNAs: negatively crossed, open, and positively crossed nucleosomes, in the order of increasing linking numbers. The fourth structure is the reversome configuration, which is assumed to be unstable in usual conditions but can be stabilized when submitted to a positive torque. The energy loss intrinsically associated to the hysteretic behavior requires the existence of an activation barrier. In our model, the barrier is related to the breaking of the docking domains which enable the nucleosome to reversome transition (18,19).
2. When a low torque Γ is applied to the magnetic bead, the reversome state cannot be reached, because chiral transition requires breaking of the docking domains. The occupation numbers n_a of each nucleosome state a ($a = n, o, p$, respectively, for negatively crossed, open, and positively crossed) are therefore given by the Boltzmann statistics as

$$n_a(\Gamma) = \frac{1}{Z} n \exp\left(\frac{F_a - 2\pi\Gamma Lk_a}{k_B T}\right), \quad (1)$$

where n is the number of positioning sequences that are actually occupied by nucleosomes ($n \leq 38$ as there are occasional gaps in the fiber), and F_a and Lk_a are, respectively, the free energy and the linking number of state a at zero torque. Z is a normalization factor which is also the system partition function. The values of F_a were estimated elsewhere (8). Note that for simplicity we write Lk_a instead of ΔLk_a throughout the text.
3. The torque increases with the number of turns imposed to the magnetic bead and eventually reaches some critical value which triggers the onset of plectonemes within the spacers DNA. Then the torque stays almost constant until plectonemes are completed and from that point, it increases dramatically. A sufficient torque is finally reached, at which value the transition toward the reversome becomes possible. Whereas the occupation numbers of the three nucleosome states are given by the Boltzmann statistics' Eq. 1, the occupation number n_r of the reversome state is given by a kinetic equation. This is due to the activation barrier that exists between the positively crossed nucleosome state and the reversome state. Denoting k_1 (respectively, k_{-1}), the positively crossed to reversome (respectively, reversome to positively crossed) rate constants, we get

$$\frac{dn_r}{dt} = k_1 n_r - k_{-1} n_p. \quad (2)$$

The barrier matches a high free energy transition state, whose linking number Lk_{tr} is intermediate between those of positively crossed nucleosome and of reversome. The rate constants are defined by the relations

$$k_1 = k_0 \exp\left(-\frac{F_{tr} - F_p - 2\pi\,\Gamma\left(Lk_{tr} - Lk_p\right)}{k_B T}\right), \quad (3)$$

$$k_{-1} = k_0 \exp\left(-\frac{F_{tr} - F_r - 2\pi\,\Gamma\left(Lk_{tr} - Lk_r\right)}{k_B T}\right). \quad (4)$$

Both rate constants k_1 and k_{-1} have been measured in Bancaud et al. (9) where the preexponential factor k_0 has been also evaluated to ~10^7 s^{-1}. This fixes the free energy of both the reversome and transition states as a function of Lk_{tr}, which is a free parameter of our model (together with n, the number of reconstituted nucleosomes). Note that, in principle, Lk_{tr} is expected to be close to the linking number Lk_p of the positively crossed state, because the barrier is associated to the breaking of the docking domains.
4. The number of turns imposed to the magnetic bead must equal the total linking number Lk of the system. Lk can in turn be decomposed as a sum of the single linking numbers Lk_a over the n reconstituted nucleosomes (20), plus the twist and the writhe of the naked DNA stretches (both flanking spacers but also parts of the DNA central fragment that are free of nucleosomes, the so-called gaps). More explicitly, we have

$$\begin{aligned} Lk &= \sum_a n_a Lk_a + Tw_{DNA} + Wr_{DNA} \\ &= \sum_a n_a Lk_a + \frac{L\Gamma}{2\pi L_P^{DNA} k_B T} + W(\Gamma), \end{aligned} \quad (5)$$

where L is the contour length of the naked DNA, L_P^{DNA} the DNA twist persistence length, and $W(\Gamma)$ the spacers DNA writhe, essentially associated to the formation of plectonemes. Note that Eq. 5 is based on an ideal geometric model of chromatin fibers. Distortions and irregularities in the chromatin constructs can lead, in principle, to major difficulties in the calculation of its topological properties (21). However, Eq. 5 leads to reasonable fits of the data (see Results and Discussion).
5. The applied torque, which is not experimentally measured, can be calculated according to the following procedure: We start at zero torque by setting the occupation numbers of the three nucleosome states according to the equilibrium condition Eq. 1, and we calculate the overall linking number Lk from Eq. 5 (with $\Gamma = 0$). The reversome occupation number n_r is initially set to zero. Then Lk is increased by a given number of turns, corresponding to the rotation imposed in the experiment between two recordings (three turns in most cases). The kinetic equations Eqs. 2–4 are then integrated over a relaxation time equal to the experimental

waiting time needed for the bead position recording. The occupation numbers n_a and the torque Γ are recalculated at the end of each integration step through Eqs. 1–5, and the values are recorded before entering a new rotation cycle. The forward (respectively, backward) curve of the hysteresis cycle is completed according to the above procedure by increasing (respectively, decreasing) Lk from 0 to Lk_{max} (respectively, from Lk_{max} to 0). Lk_{max} is the maximum number of turns applied to the bead.

6. To fit the extension rotation curves, we finally need to estimate the bead vertical position z at each step, as a function of the imposed torque. The overall extension of the complete construct includes the contributions of the naked DNA and of the parts of the DNA that are occupied by nucleosomes, forming fiber segments. The length z^{fiber} of a homogeneous fiber made of n nucleosomes of type a ($a = n, o, p$) strongly depends on the fiber geometry, which can be calculated according to the two-angle model using the computer algebra system MAPLE 9 (Maplesoft, Waterloo, Canada) (22) and can be simply written as nd_a, where d_a is the contribution per nucleosome to the fiber length and depends on the fiber geometry. Note that the fiber length is reduced at room temperature because of thermal fluctuations depending on the fiber bending persistence length, as for naked DNA (see Eq. 7, below) (23). We include this correction that, however, never exceeds 8% of the overall extension of the assembly. The total contribution of the fiber segments to the bead vertical position z is obtained by averaging the extents of homogeneous fibers of type a ($a = n, o, p$) according to their occupation numbers n_a:

$$z^{fiber} = \sum_a z_a^{fiber}(n)\frac{n_a}{n}. \quad (6)$$

The total contour length L^{DNA} of the naked part of DNA at zero torque ($\Gamma = 0$) is reduced at room temperature because of thermal fluctuations depending on its bending persistence length L_P, and can be written as (23)

$$z_0^{DNA}(n) = L^{DNA}\left(1-\frac{1}{2K}\right)\left(1+\frac{1}{64K^2}\right), \quad (7)$$

$$K = \sqrt{\frac{L_P f}{k_B T}}. \quad (8)$$

This formula can be extended to nonzero torques so as to provide a fit of the entire hysteresis cycle. Once plectoneme formation is initiated, the length of a free double-stranded DNA decreases linearly with Lk with a slope that depends on the external force and salt conditions (24). In the usual case of (partially) reconstituted fiber (i.e., when $n < 38$), the behavior of the system strongly depends on its particular configuration. We fit the slope s of the decreasing part of the experimental curve (which is roughly four times' lower than that expected for a naked DNA) from the experimental data, and use this value to model the linear part of the rotation-extension response. The DNA contribution to the overall length can finally be written as

$$\begin{aligned} z^{DNA} &= z_0^{DNA}(1 + s\,Lk_{DNA}) \\ &= z_0^{DNA}\left(1 + s\left(Lk - \sum_a n_a Lk_a\right)\right). \end{aligned} \quad (9)$$

Note that the slope s is negative.

7. Taken together, the previous considerations allow us to write the bead position z as

$$z = \sum_a \frac{n_a}{n} z_a^{fiber}(n) + z^{DNA}. \quad (10)$$

Equation 10 (together with Eqs. 6–9) allows us to evaluate the dependence of the bead position z as a function of the applied torsion Lk, and therefore to fit the experimental extension-versus-rotation curves.

Additional information regarding Materials and Methods used is provided in the Supporting Material.

RESULTS AND DISCUSSION

Chromatin assembly

Chromatin assembly was performed on a DNA construct made of 38 repeats of 601-200-bp positioning sequences (25) flanked by spacer DNAs and extended by sticking DNAs (8). Nucleosome arrays were reconstituted by stepwise dilution of a solution containing an appropriate stoichiometry of core histones (see Materials and Methods above). Because mechanical properties of chromatin fibers depend on nucleosome occupancy (8), it is necessary to verify the number and position of nucleosomes on reconstituted fibers. We checked this occupancy with gel electrophoresis of *Ava*I-digested fibers, as described in Huynh et al. (16), and concluded that almost every 601-repeat is associated at its center with one histone octamer.

We estimated that a ratio of 1.5 histone octamer per DNA repeat led to a complete reconstitution (Fig. 1 *a*). This ratio was determined on fibers containing 19 601-repeats and then applied with molecules containing 38 601-repeats (such a construct being too long to be analyzed in our electrophoretic experiments). Exceeding octamers interact with additional random-sequence DNAs of 146 bp. Transmission electron microscopy (TEM) of these chromatin fibers confirmed that particles are properly positioned and that no nucleosome clusters are observable (Fig. 1 *b*), contrary to fibers formerly made with 5S positioning sequence (9). TEM experiments also evidenced that nucleosomes are placed on 601 sequences and only very rarely on the tethering DNAs, the sequence of which does not involve any domain with known particular affinity or positioning effect.

Note also that nucleosomes can be observed in both closed (crossed) and open (uncrossed) states (see Fig. 1 *b*), although the ratio between these two conformations is expected to be biased in these experiments by the fibers adsorption on the TEM grid and the low ionic force used for proper imaging (see the Supporting Material). These TEM images showed that our assembly procedure delivers nucleosome fibers with almost full occupancy and high regularity. We applied the same protocol for the assembly of chromatosome fibers, by mixing at low ionic strength (~0.4 M NaCl) linker histone H5 (avian erythrocytes variant) with nucleosome fibers (16). This resulted in compaction of the fiber, as observed by TEM imaging (Fig. 1 *c*). Indeed, in that case nucleosomal entry/exit DNAs are maintained parallel in a stemlike structure (see *zoom picture* in Fig. 1 *c*) as previously documented (13,15). This compaction also increased the electrophoretic mobility of chromatin fibers on an agarose gel (Fig. 1 *e*), the sharp band indicating that fibers are still regularly reconstituted.

To obtain more accurate and specific controls on a fiber-by-fiber basis, we also developed a method to remove

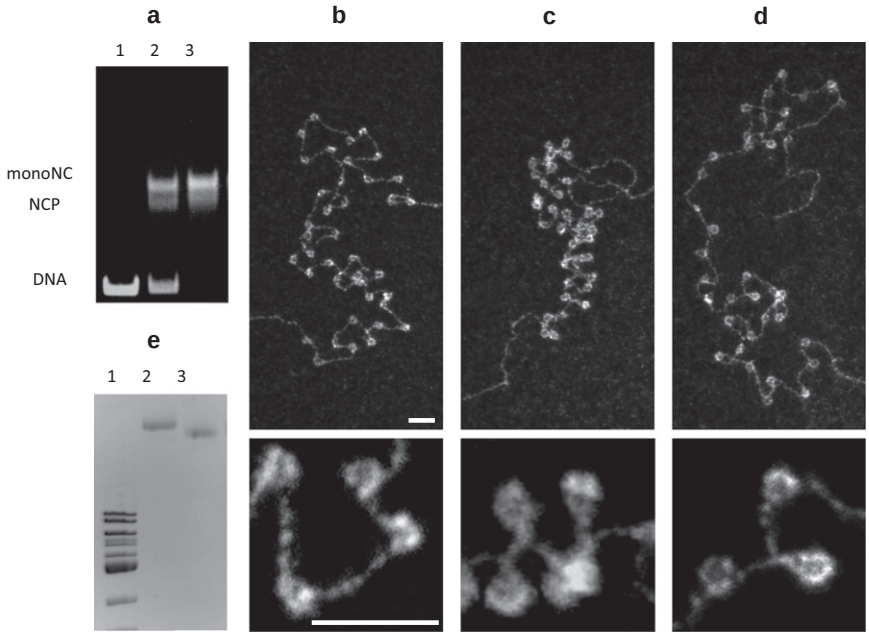

FIGURE 1 Nucleosome and chromatosome arrays. (*a*) To adjust the DNA/histone ratio we reconstituted nucleosome arrays on 19 × 200-601 by stepwise dialysis in the presence of competitor DNA (146-bp random sequence fragments). The product of *Ava*I nuclease digestion of these fibers was loaded on a polyacrylamide native gel. Binding of histone octamer to 200-bp 601 repeats is analyzed at molar input ratio of 0, 1, 1.5 histone octamers: 200-bp 601 repeat (lanes 1–3, respectively). DNA and protein-DNA complexes were visualized by staining with ethidium bromide. Position of naked 200-bp positioning sequence (DNA), competitor DNA + Octamer (NCP), and 200-bp positioning sequence + Octamer (monoNC) are indicated. The ratio determined with this technique was subsequently used for the reconstitution of the nucleosome and chromatosome fibers (38 × 200-601) manipulated in magnetic tweezers experiments. (*b*) Electron micrograph of a nucleosome fiber reconstituted on a 38 × 200-601 DNA flanked at each extremity by a spacer DNA and a sticking DNA. No nucleosome clusters are observable. Most nucleosomes are seen in an open conformation (see *zoom picture*), due to the imaging conditions (see the Supporting Material). Scale bars (*main picture* and *zoom*): 30 nm. (*c*) Electron micrograph of a chromatosome fiber. Stem motif is observable for almost every particle (see *zoom picture*), proving that linker histone is present in stoichiometric quantity. As for nucleosome fibers, no particles are present on nonpositioning flanking DNAs. Linker histones induce a shortening of the molecule. (*d*) Electron micrograph of a chromatosome fiber treated with heparin at a concentration of 1 μg/mL. Linker histones are removed, as seen from the almost total disappearance of stem motifs, whereas only a very few (<3) nucleosomes are lost. This treatment results in a more extended molecule, similar to nucleosome fibers. (*e*) 1% agarose gel electrophoresis analysis of chromatin fibers in 0.2× TB buffer (2 mM Tris, 2 mM boric acid) as described in Huynh et al. (16). Migration of 250 ng of 12 × 200-601 DNA was compared in two different conditions: reconstituted with nucleosomes (lane 2) and reconstituted with chromatosomes (lane 3). Lane 1: 10-kb DNA ladder (New England Biolabs, Ipswich, MA). Compaction induced by linker histones is revealed by the increased motility of chromatosome fibers. The ratio determined using this 12-mer template is also valid with the complete construct used for magnetic tweezers experiments (38 × 200-601 + flanking DNA). Such a short fragment is used in electrophoresis experiments because changes in migration are then detectable.

specifically linker histone from these fibers. In a previous work (9), we used heparin (a strong acidic polyelectrolyte) to remove the whole nucleosome or only H2A/H2B dimers. Here, we treated the chromatosome fibers with heparin at very low concentration (below 1 μg/mL). In these conditions, nucleosome fibers are not destabilized. On chromatosomes, this treatment yielded an elongated structure similar to that of linker histone free chromatin, as evidenced by TEM images (Fig. 1 *d*). Almost all stemlike structures disappeared while only very few (<3) nucleosomes were displaced. Moreover, such a treatment on nucleosome fibers without H5 did not seem to alter nucleosome structure , as no notable changes were observable in electrophoresis migration (data not shown) or on TEM images. Thus, we could study mechanical properties of completely and regularly reconstituted chromatin fibers with linker histone H5 and after its disruption.

Nucleosome fibers

We investigated the mechanical behavior of chromatin using magnetic tweezers (Fig. 2 *a*) (see the Supporting Material). We measured the length in low salt buffer B0 of unnicked molecules at a constant force (that we subsequently measure) and we imposed the rotation (Fig. 2 *b*). (Note that, in this setup, because the rotation is imposed by the device, the torque cannot be measured directly.) For every point in extension-rotation measurements, length is averaged over 8 s. Chromatin fibers assembled on poly-601 arrays without linker histone showed similar extension-versus-torsion responses to those obtained with 5S positioning sequences (8,9). We observed a broad apex, explained by the dynamic transition at the nucleosomal level between three different topological conformations (Fig. 2 *c*).

These conformations correspond to three possible entry/exit DNAs crossing statuses: negative, null, or positive. Nucleosomes can access these conformations by rotating around their dyad axis. Application of negative (respectively, positive) turns forces nucleosomes to adopt negative (respectively, positive) crossing. The relaxed state corresponds to equilibrium between open and crossed conformations. Once every nucleosome is in positive or negative state, the fiber undergoes an extensive shortening due to the formation of plectoneme-like structures (8). Furthermore, these regular fibers show a reproducible hysteretic behavior under large positive supercoiling (Fig. 2 *b*). This behavior has been previously reported and associated with a chiral transition of the tetramer $(H3\text{-}H4)_2$.

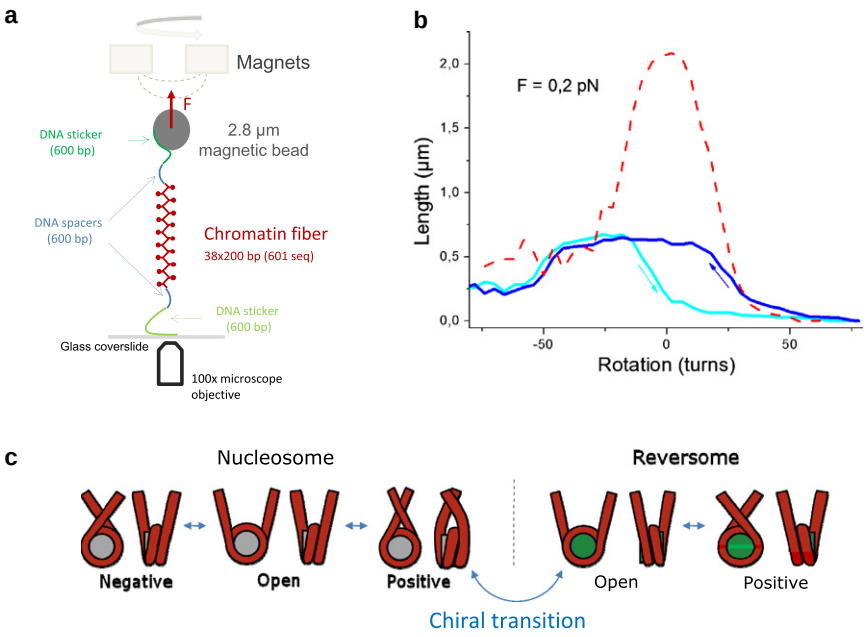

FIGURE 2 Response under topological deformation of nucleosome fibers reconstituted on 601 array. (*a*) Scheme of the magnetic tweezers setup. A single nucleosome/chromatosome array (~7.6 kbp), sandwiched between two naked DNA spacers (~600 bp each), is linked to a coated surface and to a magnetic bead. A pair of magnets placed above this molecule exerts controlled torsional and extensional constraints (17). (*b*) Extension-versus-rotation responses in buffer B0 (10 mM Tris, 1 mM EDTA, 0.1 mg/mL BSA) at a constant force of 0.2 pN. (*Light blue*) Response of a nucleosome fiber when torsion is increased from negative to positive values. In blue, response of the same fiber when torsion is decreased from positive to negative values. This cycle display a hysteresis due to the transition of individual nucleosomes to a metastable particle called a reversome. The reversome consists in the rightward wrapping of DNA around the histone octamer. This reproducible hysteresis is due to the reversible trapping of one positive turn in every reversome during chiral transition (9). (*Red*) Response of the corresponding naked DNA after a treatment with heparin at a concentration of 500 μg/mL. The shift in topology after nucleosome removal is consistent with the topological deformation of -1 turn per nucleosome. (*c*) Model of the nucleosome behavior under topological deformation. Under moderate torsion, nucleosome can adapt its topology according to the three-state model (8). Extensive positive topological deformation induces a chiral transition that leads to a reversome, in which DNA is wrapped in a rightward manner around histone octamer. This state can exist in two topological states—open or positively crossed. Topological adaptation at the nucleosomal level gives rise to a remarkable torsional elasticity of chromatin fibers compared to naked DNA (8,9).

This transition leads to an altered structure of the nucleosome forming a metastable particle called a reversome (9) or R-octasome (18). During the transition, every nucleosome contributes to the trapping of one positive turn (the mean topology shift per nucleosome is estimated to -1.0 ± 0.1 turn). Torsion is captured by individual nucleosomes instead of being trapped in a plectonemic loop. This striking dynamics is observed with high affinity sequence 601, and is very similar to that previously obtained with 5S fibers, indicating that the strong positioning effect of 601 sequences does not result in a significant stiffening of the structure from a topological point of view.

Subsequent to histone removal (injection of 500 μg/mL heparin), we measured the response of the corresponding naked DNA. This provides an absolute reference for the topological states of the fibers, because one nucleosome adds, on average, ~-1 turn. We can thus confirm, a posteriori, the number of nucleosomes present on the studied fiber, evidenced by the lengthening of the fiber. The reference is determined using the rotation corresponding to the maximal extension of the naked DNA molecule.

We occasionally observed a loss of a few particles during the performance of magnetic tweezer experiments. This loss is expected to be due to the duration of the experiment, to the extensional and torsional constraints experienced by the fiber during buffer exchanges and fiber manipulation, and to interactions with surfaces. Studied fibers typically comprised between 25 and 38 nucleosomes.

Torsional studies of chromatosome fibers at moderate torsional strains

In the same low salt buffer, we manipulated chromatin fibers fully saturated with linker histone H5 at a constant force below 0.5 pN. Such a load is not sufficient to destabilize linker histones; indeed previous single-molecule force spectroscopy experiments showed that the detachment of linker histones occurs at a force higher than 4.5 pN (7). Biochemical experiments proved that individual chromatosomes can adopt two different topological conformations (15,26)—positively crossed and negatively crossed. Binding of linker histone suppressed the open conformation, because entry/exit DNAs are maintained parallel in close contact in a stem-like structure. However, our experiments confirm that chromatosomes can still flip from negative to positive crossing statuses by rotating around dyad axis (Fig. 3 *a*, *light-blue curve*) as expected from biochemical data (15). Qualitatively, we observed a large apex indicating that chromatosomes adapt their topology to rotational strains (Fig. 3 *b*). In that case, it corresponds to a direct transition between negative and positive states.

Behavior of chromatosome fibers upon high positive torsional strains

Surprisingly, upon high torsional strain, chromatosomes are still able to undergo a chiral transition toward a metastable

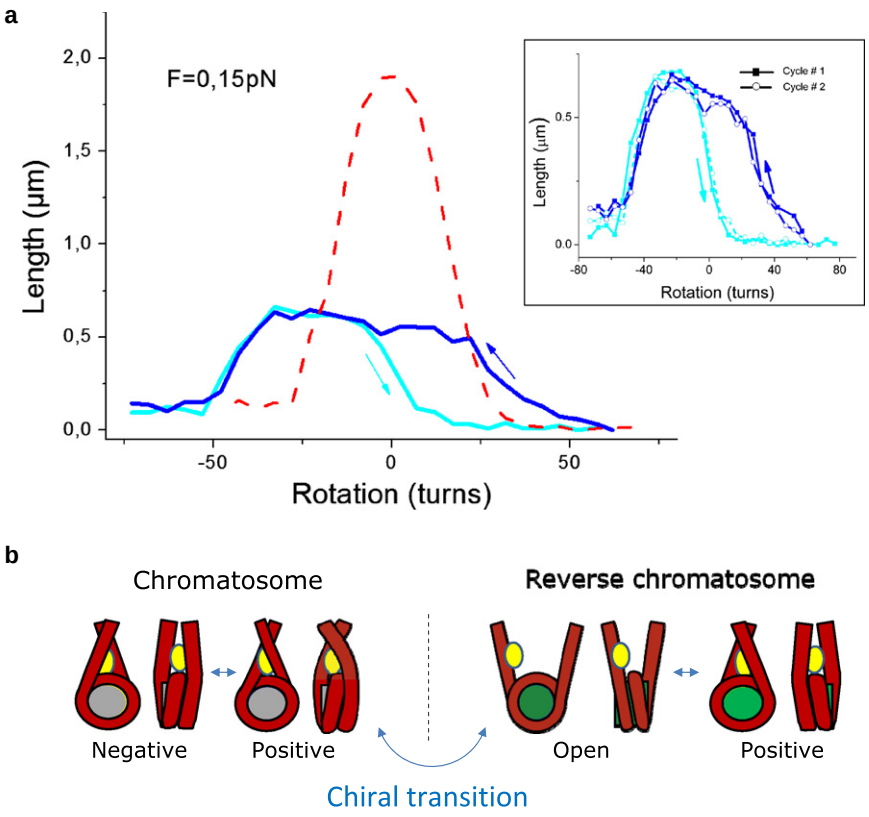

FIGURE 3 Response under topological deformation of a chromatosome fiber. (*a*) Extension-versus-rotation responses in buffer B0 at a constant force of 0.15 pN. (*Light blue*) Response of a chromatosome fiber when torsion is increased from negative to positive values. (*Blue*) Response of the same fiber when torsion is decreased from positive to negative values. This cycle displays the same hysteretic behavior as in the case of nucleosome fibers. It indicates that the chiral transition described previously is still possible when entry/exit DNAs are locked by linker histone. (*Red*) Response of the corresponding naked DNA after a treatment with heparin at a concentration of 500 μg/mL. The shift in topology after chromatosome removal is ~−1.4 turns per particle. It reflects a different repartition of the two states of the chromatosome compared to the three states of the nucleosome and/or of their topologies. (*Inset*) Two successive hysteresis cycles are presented (*light blue*, forward curves; *blue*, backward curves). These two cycles are identical, thus proving that linker histones are not ejected from the fiber when submitted to an extensive positive supercoiling. (*b*) Models of the states accessible for the chromatosome under topological constraints. Under moderate deformation, chromatosomes can be found under the negatively or positively crossed conformation, explaining the large apex observable (*light-blue curve* in panel *a*). Extensive positive supercoiling induces the formation of reverse chromatosomes responsible for the trapping of one positive turn per particle. This value is comparable to the one measured for nucleosomes fibers. It could be a clue that reversome conformation is identical in the two cases and that linker histone does not participate in that structure. However, linker histone is not ejected during chiral transition, because the hysteresis is reproducible, this protein being still attached to the reversomes.

state with positive supercoiling, similar to that observed for nucleosome fibers (Fig. 3 *b*, *dark-blue curve*). Application of a large positive supercoiling leads to a transition to reverse chromatosomes, as seen from the appearance of a hysteretic behavior similar to that observed with nucleosome arrays (9). The high positive supercoiling leading to this hysteresis does not induce the ejection of linker histones; indeed after one cycle the forward curve (obtained by increasing the number of turns from negative to positive values) is not affected, proving that H5 histones are still present in the fiber and properly interacting with nucleosomes (Fig. 3 *a*, *inset*). Therefore, this chiral transition is still possible with entry/exit DNAs locked in antiparallel conformation and does not induce ejection of linker histones, as the forward curve is not modified after one cycle.

This is rather surprising at first glance, because linker histone is thought to act as a lock for entry and exit DNA, apparently preventing the reorganization of nucleosomal DNA, thus the chiral transition as depicted before (9) (see also (27) and supplemental movie therein). We propose two different models explaining the chiral transition of chromatosomes.

First, the high torque applied may induce the complete breaking of the interaction between linker histone and entry/exit DNAs, H5 being still attached to one of the two strands because of the strong interaction in low salt buffer. Close contact of entry/exit DNA in the canonical nucleosome leads back to the attachment of linker histone to both DNA. Alternatively, the torque may induce partial opening of the stem, reducing steric hindrance so that chiral transition can occur.

Comparison with nucleosome fibers

We injected in the flow cell a low concentration solution of heparin (1 μg/mL), so that we remove linker histones. We can then compare a chromatosome fiber with its corresponding nucleosome fiber. Results are presented in Fig. 4. As discussed above, hysteretic behaviors of chromatosome fiber (*left panel*) and of its corresponding nucleosome fiber (*right panel*) are similar. In the central panel, we present in pink (respectively, *purple*) the forward curve of the chromatosome (respectively, nucleosome) fiber. We observed on these extension-versus-rotation responses an increase in length (δL on Fig. 4). This is due in part to detachment of DNA involved in the stem structure and, also, to the loss of a few nucleosomes (see next section). Moreover, we noticed a significant, yet slight, shift in topology, i.e., a shift of the whole curve toward positive values of rotation (δR on Fig. 4). This shift reflects a change in topology of the states

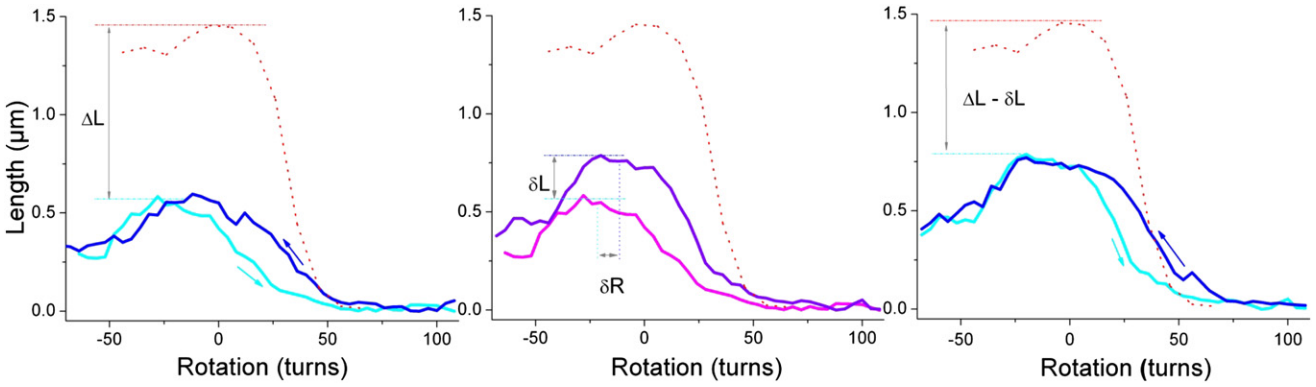

FIGURE 4 Response under topological deformation of a chromatosome fiber after treatment with heparin. We show a comparison of extension-versus-rotation of a chromatosome fiber (*left*) and its corresponding nucleosome fiber (*right*). Linker histones were removed specifically by injecting heparin at a concentration of 1 μg/mL in buffer B0. Both exhibit the typical hysteretic behavior of chromatin fibers. (*Middle panel*) Comparison between forward curves of the chromatosome fiber (*pink*) and the nucleosome fiber (*purple*). One can observe a lengthening (δL) due to removal of linker histones which is ~200 nm. A slight shift in topology (δR), i.e., in the linking number, is also observable toward positive values after linker histone removal. It is estimated to be ~0.5 per particle. (*Red*) Response of the corresponding naked DNA (the asymmetry of its response is due to the denaturation of DNA occurring under negative supercoiling (17)).

accessible to the nucleosome upon association with linker histone H5 (15) and, again, the loss of a few nucleosomes.

Comparison with computer modeling

In absence of H5, the fit of the nucleosome fibers is obtained through the procedure delineated in Materials and Methods (Eq. 10), where the linking number Lk_a and length contribution d_a of each nucleosome state a are deduced from the fiber geometry according to the two-angle model (20,22). For the case of the reversome structure, which is not completely resolved, we assume a mirror image of the positively crossed state nucleosome. The resulting linking numbers are:

$$Lk_n = -1.54; Lk_o = -0.54; Lk_p = -0.34; \text{ and } Lk_r = 0.60.$$

Once these values are included in the model, the only free parameters in the fit are the actual number n of nucleosomes reconstituted on the central fragment of the DNA template (i.e., the 38 × 200 bp-601 positioning sequence) and the position of the transition barrier (the barrier energy being then determined through Eqs. 3 and 4).

The position of the barrier is a quite sensitive parameter determining the stability of the positive (respectively, reversome) states during the transition and consequently the shape of the hysteresis cycle (data not shown). The fitting of the experimental data leads to $Lk_{tr} = -0.25 \pm 0.05$. The determination of the number of nucleosomes in the array is facilitated by the fact that it strongly influences the bead vertical position z. Indeed, for each lost nucleosome (or gap), the naked DNA contour length is increased by ~70 nm (corresponding to the added 200 bp), whereas the corresponding fiber length is only slightly decreased (by ~4 nm in average at low torque). The fit of the hysteretic curve therefore allows us to adjust the parameter n quite precisely (see Fig. 5).

Once we have fitted the rotation-extension curves for one particular nucleosome array (Fig. 5 *a*), we can consider the corresponding chromatosome fiber. In this case, the open state is suppressed (15), but the reversome state is probably conserved, as indicated by the existence of hysteresis. The chromatosome precise structure being unknown, linking number and fiber length contributions of the nucleosome in each state a cannot be calculated on the basis of the two-angle model. However, TEM imaging suggests that the fibers are strongly compacted by H5, so we temptingly assume a minimal contribution length of 2 nm for any chromatosome state. Within this hypothesis, the array extent at zero torque can be easily calculated and compared to the experimental results, this leading to an estimation of n.

As displayed schematically in Fig. 5 *b*, the difference in length between the nucleosome fiber (which best fits the hysteresis cycle on Fig. 5 *a*) and the chromatosome fiber (which best fits the hysteresis cycle on Fig. 5 *c*) can only be explained by assuming that two nucleosomes are lost during the heparin treatment. Once fixed, the number of nucleosomes n, the remaining free parameters for the fitting procedure in the case of chromatosomes, are the linking number contributions $Lk(chrom)_a$ of the states $a = n, p, r$. The fit of Fig. 5 *c* is obtained by translating the values of all the corresponding nucleosome states Lk_a by one and the same negative amount:

$$Lk(chrom)_a = Lk_a - 0.5.$$

This suggests that H5 binding on the nucleosome is accompanied by some further wrapping of the DNA on the histone octamer, thus inducing a more negative linking number of the chromatosome states with respect to the nucleosome ones, as observed previously (15).

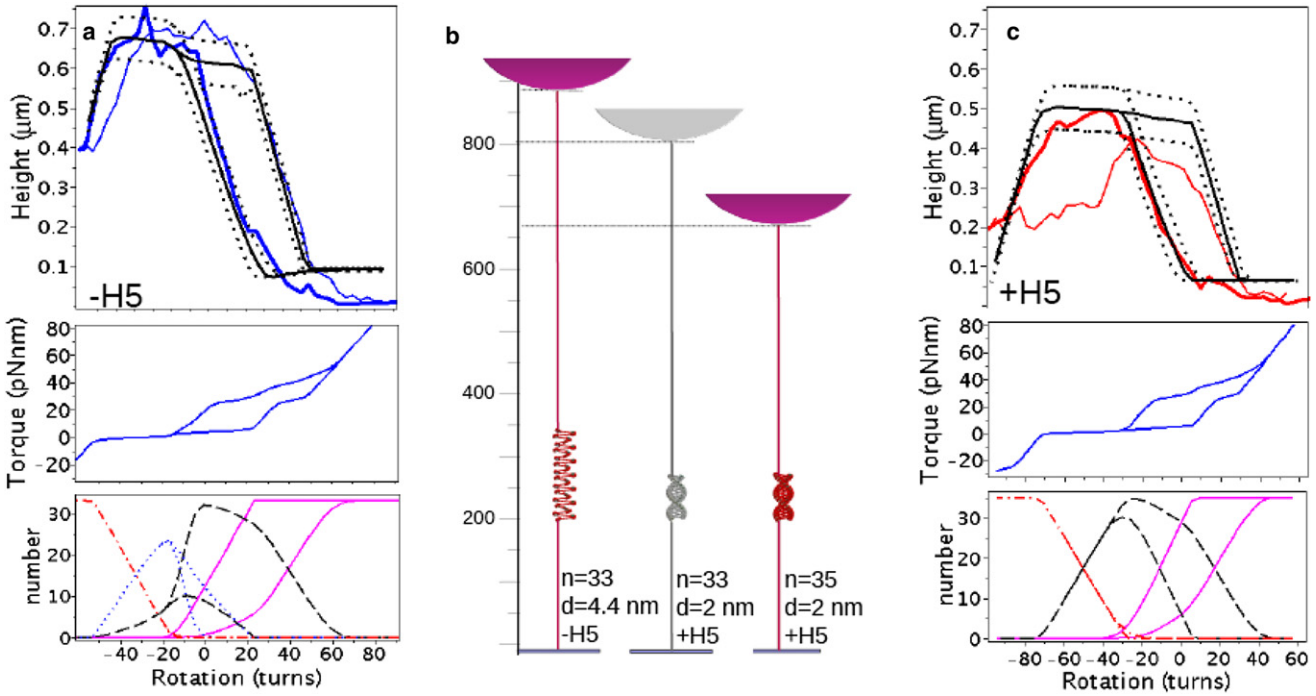

FIGURE 5 Fit of the nucleosome and chromatosome hysteresis cycles. (*a*) (*Top*, in *blue*) hysteresis cycle of the nucleosome construct obtained after linker histones removal by heparin treatment on the initial chromatosome construct (hysteresis cycle on panel *c*); a fit of the response curve theoretically obtained with a fiber containing $n = 33$ nucleosomes is displayed (*black solid line*) together with the response curves obtained when using $n = 32$ or $n = 34$ (*black dotted lines*). (*Middle*) Evolution of the torque experienced by the fiber during the same hysteresis cycle. (*Bottom*) Evolution of the populations of the different nucleosome states during the same hysteresis cycle. (*Red/dot-dashed line*) Negative; (*blue/dotted line*) open; (*black*, *dashed line*) positive; (*magenta/solid line*) reversome. (*b*) Comparison of the stretched extension of a nucleosome construct with $n = 33$ nucleosomes (*left sketch*) with those of two chromatosome constructs with $n = 35$ (*right sketch*) and $n = 33$ (*gray/central sketch*) chromatosomes. (*c*) (*Top*, *red*) Hysteresis cycle obtained for the initial chromatosome construct; a fit of the fiber with $n = 35$ chromatosomes is displayed (*black/solid line*) together with the response curves theoretically obtained by using $n = 34$ or $n = 36$ (*black dotted lines*). (*Middle*) Evolution of the torque experienced by the fiber during the same hysteresis cycle. (*Bottom*) Evolution of the populations of the different nucleosome states during the same hysteresis cycle. (*Red/dot-dashed line*) Negative; (*black/dashed line*) positive; (*magenta/solid line*) reversome. The comparison of the maximum extension of the two constructs as measured in panels *a* and *c* shows that two nucleosomes have been lost during the heparin treatment. Indeed, the observed shortening of the overall length cannot be explained only by the fiber compaction induced by the linker histone (*gray central sketch* in *b*) but is compatible with the addition of two nucleosomes and the corresponding reduction of the naked DNA (*right sketch* in panel *b*).

We also computed the torque experienced by the fiber (see Fig. 5). Interestingly, the torque corresponding to the first nucleosome to reversome transition is close to 20 pN nm in both experiments (with and without H5). We therefore conclude that the torque necessary to unbind H5 from one linker DNA is less than this value. Consequently, H5 seems not to hamper the transition. On the other hand, because the initial fiber is recovered after one complete hysteresis cycle (see Fig. 3, *inset*), H5 is not lost in the solution, and the most probable explanation is that it remains bound to the other linker DNA.

SUMMARY AND CONCLUSIONS

We studied here the response of chromatosome fibers upon torsional constraints. At moderate strains, these fibers have a resilience qualitatively similar to that of nucleosome fibers. This behavior was well fitted by a model in which individual chromatosomes transit between a positively crossed and a negatively crossed state. Both states have entry-exit DNA stems close to each other, and are thus compatible with the presence of a linker histone between them.

More surprisingly, chromatosomes seem able to undergo a chiral transition toward a positive state, similar to that recently observed for nucleosomes upon strong positive strain. The linker histone is not lost during the transition, suggesting that chromatosome fibers are able, as nucleosome ones, to store large positive supercoiling upon torsional stresses. The fact that nucleosomes as well as chromatosomes can adapt their conformation to topological constraints provides a further demonstration of chromatin plasticity sustained by the conformational dynamics of its constituents (28).

In linker-histone-containing fibers the chromatosome-to-reversome transition occurred for a similar amount of positive turns applied, i.e., for torque similar to those at which nucleosome-to-reversome transition occurs (9). These chiral

transitions involve torsional stresses easily achievable by DNA-twisting enzymes, such as polymerases (2). The conservation in chromatosome fibers of the strong resilience and chiral transition is a further argument in favor of the occurrence of such phenomena in vivo, and of their biological relevance. A first obvious physiological utility would be the role of torsion buffers, keeping chromatin's torsional stress at a constant level, lower than the stall stress of polymerases during their progression.

This would thus allow efficient operation of a larger number of polymerases on the same strand, without requiring any ejection of core or linker histones, i.e., with a minimal alteration of the structure. It has been shown that prior topoisomerases relax the topological deformation in vivo, and stress is accumulated in the fiber (29)—thus enforcing the idea that chromatin itself must accommodate these constraints (30). Modifications of histone tails are now recognized as major epigenetic factors, so that allowing for the action of polymerases by mere conformational changes in the chromatosomes with any histone removal, would indeed be a key factor for the maintenance of the epigenetic code.

Because the chiral transition of nucleosomes has only been recently described and that of chromatosomes is reported here for the first time (to our knowledge), little is known so far about the precise structure of the positive state. Experimental work on centromeric chromatin (11) and recent computer modeling (27) suggest that they involve histone-histone and histone-DNA interaction energies significantly different from those of conventional chromatosomes. Then, this chiral transition may also have more subtle effects, regarding the accessibility of DNA or nucleosomes to regulatory proteins.

Linker histones have many competitors for nucleosome binding in vivo, among which are high mobility group proteins, which are generally thought to give chromatin more plasticity and in particular to increase its transcriptional potential (31). A temporary destabilization of linker histones by torsional stress may thus activate their exchange by competitors, and exert positive or negative feedback effects on chromatin plasticity. Because torsional stress can propagate along chromatin, transitions of the chromatosomes such as those observed here could thus provide a very simple mechanical way to perform, in a short passage of time, information transmission and signaling over long distances.

SUPPORTING MATERIAL

Additional materials and methods are available at http://www.biophysj.org/biophysj/supplemental/S0006-3495(11)00468-1.

We thank Vincent Croquette and Ariel Prunell for discussion and experimental help.

This work was financially supported by Agence Nationale de la Recherche FdV project "FarcC" and Agence Nationale de la Recherche PNANO project "Chromatopinces".

REFERENCES

1. Cozzarelli, N. R., G. J. Cost, …, J. E. Stray. 2006. Giant proteins that move DNA: bullies of the genomic playground. *Nat. Rev. Mol. Cell Biol.* 7:580–588.
2. Lavelle, C. 2009. Forces and torques in the nucleus: chromatin under mechanical constraints. *Biochem. Cell Biol.* 87:307–322.
3. Bennink, M. L., S. H. Leuba, …, J. Greve. 2001. Unfolding individual nucleosomes by stretching single chromatin fibers with optical tweezers. *Nat. Struct. Biol.* 8:606–610.
4. Brower-Toland, B. D., C. L. Smith, …, M. D. Wang. 2002. Mechanical disruption of individual nucleosomes reveals a reversible multistage release of DNA. *Proc. Natl. Acad. Sci. USA.* 99:1960–1965.
5. Cui, Y., and C. Bustamante. 2000. Pulling a single chromatin fiber reveals the forces that maintain its higher-order structure. *Proc. Natl. Acad. Sci. USA.* 97:127–132.
6. Pope, L. H., M. L. Bennink, …, J. F. Marko. 2005. Single chromatin fiber stretching reveals physically distinct populations of disassembly events. *Biophys. J.* 88:3572–3583.
7. Kruithof, M., F. T. Chien, …, J. van Noort. 2009. Single-molecule force spectroscopy reveals a highly compliant helical folding for the 30-nm chromatin fiber. *Nat. Struct. Mol. Biol.* 16:534–540.
8. Bancaud, A., N. Conde e Silva, …, J. L. Viovy. 2006. Structural plasticity of single chromatin fibers revealed by torsional manipulation. *Nat. Struct. Mol. Biol.* 13:444–450.
9. Bancaud, A., G. Wagner, …, A. Prunell. 2007. Nucleosome chiral transition under positive torsional stress in single chromatin fibers. *Mol. Cell.* 27:135–147.
10. Hamiche, A., V. Carot, …, A. Prunell. 1996. Interaction of the histone (H3-H4)2 tetramer of the nucleosome with positively supercoiled DNA minicircles: potential flipping of the protein from a left- to a right-handed superhelical form. *Proc. Natl. Acad. Sci. USA.* 93:7588–7593.
11. Furuyama, T., and S. Henikoff. 2009. Centromeric nucleosomes induce positive DNA supercoils. *Cell.* 138:104–113.
12. Bednar, J., R. A. Horowitz, …, C. L. Woodcock. 1998. Nucleosomes, linker DNA, and linker histone form a unique structural motif that directs the higher-order folding and compaction of chromatin. *Proc. Natl. Acad. Sci. USA.* 95:14173–14178.
13. Hamiche, A., P. Schultz, …, A. Prunell. 1996. Linker histone-dependent DNA structure in linear mononucleosomes. *J. Mol. Biol.* 257: 30–42.
14. Sivolob, A., C. Lavelle, and A. Prunell. 2009. Flexibility of nucleosomes on topologically constrained DNA. *In* Mathematics of DNA Structure, Function, and Interactions. C. J. Benham, S. Harvey, W. K. Olson, D. W. L. Sumners, and D. Swigon, editors. Springer, New York. 251–292.
15. Sivolob, A., and A. Prunell. 2003. Linker histone-dependent organization and dynamics of nucleosome entry/exit DNAs. *J. Mol. Biol.* 331:1025–1040.
16. Huynh, V. A., P. J. Robinson, and D. Rhodes. 2005. A method for the in vitro reconstitution of a defined "30 nm" chromatin fiber containing stoichiometric amounts of the linker histone. *J. Mol. Biol.* 345: 957–968.
17. Strick, T. R., J. F. Allemand, …, V. Croquette. 1996. The elasticity of a single supercoiled DNA molecule. *Science.* 271:1835–1837.
18. Zlatanova, J., T. C. Bishop, …, K. van Holde. 2009. The nucleosome family: dynamic and growing. *Structure.* 17:160–171.
19. Bohm, V., A. R. Hieb, …, J. Langowski. 2011. Nucleosome accessibility governed by the dimer/tetramer interface. *Nucl. Acids Res.*, 2010 Dec 21. [Epub ahead of print].
20. Barbi, M., J. Mozziconacci, and J. M. Victor. 2005. How the chromatin fiber deals with topological constraints. *Phys. Rev. E Stat. Nonlin. Soft Matter Phys.* 71:031910.
21. Neukirch, S., and E. L. Starostin. 2008. Writhe formulas and antipodal points in plectonemic DNA configurations. *Phys. Rev. E Stat. Nonlin. Soft Matter Phys.* 78:041912.

22. Ben-Haïm, E., A. Lesne, and J. M. Victor. 2001. Chromatin: a tunable spring at work inside chromosomes. *Phys. Rev. E Stat. Nonlin. Soft Matter Phys.* 64:051921.

23. Moroz, J. D., and P. Nelson. 1997. Torsional directed walks, entropic elasticity, and DNA twist stiffness. *Proc. Natl. Acad. Sci. USA.* 94:14418–14422.

24. Neukirch, S. 2004. Extracting DNA twist rigidity from experimental supercoiling data. *Phys. Rev. Lett.* 93:198107.

25. Lowary, P. T., and J. Widom. 1998. New DNA sequence rules for high affinity binding to histone octamer and sequence-directed nucleosome positioning. *J. Mol. Biol.* 276:19–42.

26. Sivolob, A., and A. Prunell. 2004. Nucleosome conformational flexibility and implications for chromatin dynamics. *Philos. Transact. A Math. Phys. Eng. Sci.* 362:1519–1547.

27. Lavelle, C., P. Recouvreux, …, J. M. Victor. 2009. Right-handed nucleosome: myth or reality? *Cell.* 139:1216–1218.

28. Lavelle, C., and A. Prunell. 2007. Chromatin polymorphism and the nucleosome superfamily: a genealogy. *Cell Cycle.* 6:2113–2119.

29. Kouzine, F., S. Sanford, …, D. Levens. 2008. The functional response of upstream DNA to dynamic supercoiling in vivo. *Nat. Struct. Mol. Biol.* 15:146–154.

30. Lavelle, C. 2008. DNA torsional stress propagates through chromatin fiber and participates in transcriptional regulation. *Nat. Struct. Mol. Biol.* 15:123–125.

31. Catez, F., H. Yang, …, M. Bustin. 2004. Network of dynamic interactions between histone H1 and high-mobility-group proteins in chromatin. *Mol. Cell. Biol.* 24:4321–4328.

Linker histones incorporation maintains chromatin fiber plasticity

Pierre Recouvreux, Christophe Lavelle, Maria Barbi, Natalia

Conde e silva, Eric le Cam, jean-marc Victor, and Jean-Louis Viovy

Electron microscopy

Transmission electron microscopy visualization was performed as in (9). Briefly, 5µl of reconstituted nucleosome arrays at 1-5nM in TE (10 mM Tris-HCl [pH 7.5], 1 mM EDTA) were deposited onto a 600-mesh copper grid covered with a thin carbon film, activated by glow-discharge in the presence of pentylamine ; grids were washed with aqueous 2% (w/v) uranyl acetate, dried and observed in the annular darkfield mode using a Zeiss 902 electron microscope ; images were captured with a MegaviewIII CCD camera. Note that spreading in low salt buffer (TE) and interactions with carbon layer favor repulsion between DNA strands, so that most nucleosomes appear in open conformation on TEM images.

Magnetic tweezers experiments

A poly-di-methylsiloxane (PDMS; Dow-Corning, Midland, MI) flow cell with a 2-mm-wide and 80-µm-high channel was constructed. This microfluidic cell was mounted on a glass coverslip treated with silane SigmaCote (Sigma Aldrich, Saint-Louis, MO). The surface-coating was performed inside the channel with nonspecific binding of anti-digoxigenin (Roche Applied Science, Basel, Switzerland) for 1 h at 37°C, followed by overnight BSA blocking. The PDMS flow cell was placed beneath two NdFeB permanent magnets (HPMG, China) separated by 0.8 mm. Images were grabbed by a CCD camera CV-A10GE (JAI, Copenhagen, Denmark). Moving the magnets up and down allows application of a force in the range 0.1 - 15 pN. The topological constraint was controlled by rotation of the magnets about the vertical axis. Magnets actuation and bead position measurement were done using electronics and software developed by PicoTwist (Saint-Romain de Coppey, France).

Just before the experiment, 1 ng of chromatin, previously diluted to 10 µl with buffer B0, was mixed with 100 µg of 2.8-mm-diameter streptavidin-coated magnetic beads (Invitrogen, Carlsbad,CA). The solution was aspirated into the cell by a syringe pump. After an incubation of 30 minutes buffer B0 was flushed into the microchannel to rinse out non attached beads. Force is then set by the vertical position of magnets, after the experiment the applied force is determined precisely thanks to the measurement of brownian fluctuations of the bead (17). The rotation-extension response of a fiber consists in the measurement of the

vertical position of the bead in function of the rotation of the magnets (at a constant force). This length is measured by an averaging over a time window of 4 to 8 seconds.